SINTEF
PROCEEDINGS
2

Proceedings of the 12th International Conference on Computational Fluid Dynamics in the Oil & Gas, Metallurgical and Process Industries

Progress in Applied CFD – CFD2017

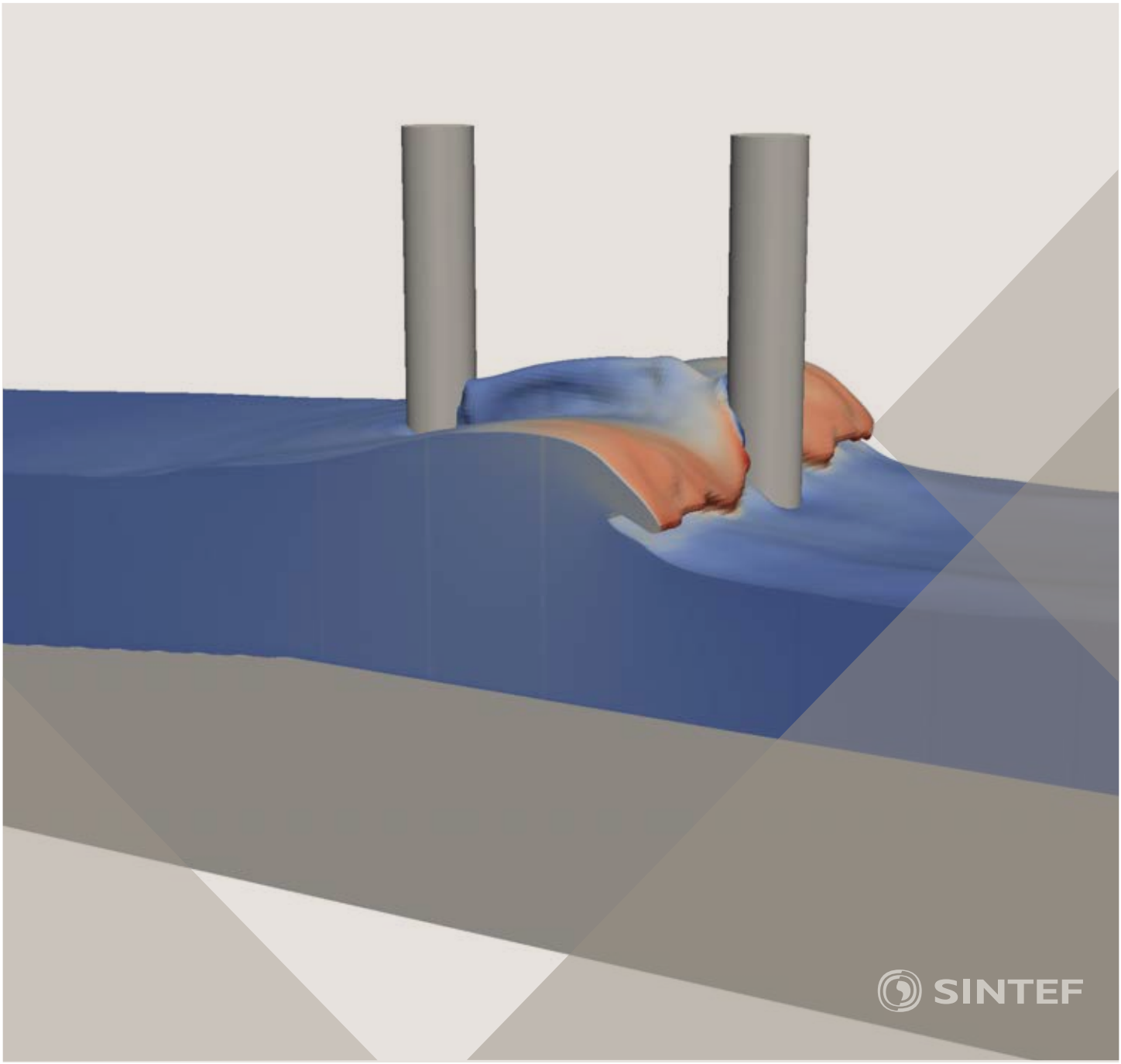

SINTEF Proceedings

Editors:
Jan Erik Olsen and Stein Tore Johansen

Progress in Applied CFD – CFD2017

Proceedings of the 12th International Conference on Computational Fluid Dynamics in the Oil & Gas, Metallurgical and Process Industries

SINTEF Academic Press

SINTEF Proceedings no 2
Editors: Jan Erik Olsen and Stein Tore Johansen
Progress in Applied CFD – CFD2017
Selected papers from 10th International Conference on Computational Fluid Dynamics in the Oil & Gas, Metallurgical and Process Industries

Key words:
CFD, Flow, Modelling

Cover, illustration: Arun Kamath

ISSN 2387-4295 (online)
ISBN 978-82-536-1544-8 (pdf)

SINTEF Academic Press
Address: Forskningsveien 3 B
PO Box 124 Blindern
N-0314 OSLO
Tel: +47 73 59 30 00
Fax: +47 22 96 55 08

www.sintef.no/byggforsk
www.sintefbok.no

SINTEF Proceedings
SINTEF Proceedings is a serial publication for peer-reviewed conference proceedings on a variety of scientific topics.
The processes of peer-reviewing of papers published in SINTEF Proceedings are administered by the conference organizers and proceedings editors. Detailed procedures will vary according to custom and practice in each scientific community.

PREFACE

This book contains all manuscripts approved by the reviewers and the organizing committee of the 12th International Conference on Computational Fluid Dynamics in the Oil & Gas, Metallurgical and Process Industries. The conference was hosted by SINTEF in Trondheim in May/June 2017 and is also known as CFD2017 for short. The conference series was initiated by CSIRO and Phil Schwarz in 1997. So far the conference has been alternating between CSIRO in Melbourne and SINTEF in Trondheim. The conferences focuses on the application of CFD in the oil and gas industries, metal production, mineral processing, power generation, chemicals and other process industries. In addition pragmatic modelling concepts and bio-mechanical applications have become an important part of the conference. The papers in this book demonstrate the current progress in applied CFD.

The conference papers undergo a review process involving two experts. Only papers accepted by the reviewers are included in the proceedings. 108 contributions were presented at the conference together with six keynote presentations. A majority of these contributions are presented by their manuscript in this collection (a few were granted to present without an accompanying manuscript).

The organizing committee would like to thank everyone who has helped with review of manuscripts, all those who helped to promote the conference and all authors who have submitted scientific contributions. We are also grateful for the support from the conference sponsors: ANSYS, SFI Metal Production and NanoSim.

Stein Tore Johansen & Jan Erik Olsen

Organizing committee:

Conference chairman: Prof. Stein Tore Johansen
Conference coordinator: Dr. Jan Erik Olsen
Dr. Bernhard Müller
Dr.Sigrid Karstad Dahl
Dr.Shahriar Amini
Dr.Ernst Meese
Dr.Josip Zoric
Dr.Jannike Solsvik
Dr.Peter Witt

Scientific committee:

Stein Tore Johansen, SINTEF/NTNU
Bernhard Müller, NTNU
Phil Schwarz, CSIRO
Akio Tomiyama, Kobe University
Hans Kuipers, Eindhoven University of Technology
Jinghai Li, Chinese Academy of Science
Markus Braun, Ansys
Simon Lo, CD-adapco
Patrick Segers, Universiteit Gent
Jiyuan Tu, RMIT
Jos Derksen, University of Aberdeen
Dmitry Eskin, Schlumberger-Doll Research
Pär Jönsson, KTH
Stefan Pirker, Johannes Kepler University
Josip Zoric, SINTEF

CONTENTS

ESTIMATION OF FLOW RATES AND PARAMETERS IN TWO-PHASE STRATIFIED AND SLUG FLOW BY AN ENSEMBLE KALMAN FILTER

Marco FERRARI[1*], **Arianna BONZANINI**[2†], **Gianni ARIOLI**[1‡], **Pietro POESIO**[2§]

[1]Politecnico di Milano, Department of Mathematics, 20133 Milan, ITALY

[2]Universita' degli Studi di Brescia, Department of Mechanical and Industrial Engineering, 25123 Brescia, ITALY

[*] E-mail: marco2.ferrari@polimi.it
[†] E-mail: a.bonzanini001@unibs.it
[‡] E-mail: gianni.arioli@polimi.it
[§] E-mail: pietro.poesio@unibs.it

ABSTRACT

Data assimilation methods were introduced to reduce production costs and to optimize processes in different industrial fields, such as oil & gas reservoir industry or transport of multiphase flows in pipelines. In flow assurance, these methods, called also soft-sensing techniques, allow to avoid the use of expensive and complex multiphase meters to measure some flow characteristics. Moreover, they allow the estimation of some flow parameters, whose actual values are unknown. Using these techniques, flow meters may be substituted by numerical simulations that solve a real-time dynamic model.

Among data assimilation methods, sequential filtering techniques allow flow estimation using a mathematical recursive filter where the estimated state of the physical model is updated in real-time through a comparison with few available and easy to obtain measurements of the actual system. If an explicit matrix structure of the model is available, the Extended Kalman filter (EKF) can be used as a recursive filter; otherwise, in the case of a more complex physical model, the Ensemble Kalman filter (EnKF), that is a stochastic extension of the original Kalman filter, can be used in combination with a numerical code to estimate various pieces of information of a multiphase flow in pipe.

Previous Authors (see Gryzlov et al. (2010)) used the Extended or the Ensemble Kalman filter in combination with the simplified one-dimensional no-pressure wave and drift-flux models to estimate the inlet flow rate or some correlation parameters in liquid/gas two-phase flow.

In this work, the application of the Ensemble Kalman filter to the more complex Two-Fluid model for two-phase flow is investigated. The possibility to extend flow rate estimations to simulations where a flow regime transition from stratified to slug flow occurs, simulated with a one-dimensional slug capturing numerical code previously developed, is shown. The estimation of the pipe diameter by the real-time soft-sensing technique is performed in order to show the possibility of evaluating the presence of possible pipe restrictions or obstructions along the pipe due to wax deposition, solid phase scaling or other similar processes, without the use of ad-hoc physical model or invasive examination of the pipe. All the measurements used in this work for the soft-sensing process are obtained from previous numerical simulations of artificial actual systems kept as reference.

Keywords: Multiphase pipeline transport, Oil & Gas .

NOMENCLATURE

Greek Symbols

α	Volume fraction.
ρ	Density, $[kg/m^3]$.
μ	Dynamic viscosity, $[Pa \cdot s]$.
θ	Inclination angle, $[rad]$.
τ	Shear stress, $[N/m^2]$.
Δ	Interval.
υ	Measurements Gaussian error.

Latin Symbols

x	Axial length coordinate, $[m]$.
t	Time coordinate, $[s]$.
p	Pressure, $[Pa]$.
u	Phase velocity, $[m/s]$.
g	Gravity acceleration, $[m/s^2]$.
F	Frictional force, $[N/m^3]$.
r_p	Pressure relaxation parameter, $[(Pa \cdot s)^{-1}]$.
c	Speed of sound, $[m/s]$.
f	Friction factor.
Re	Reynolds number, $[m/s]$.
D	Pipe diameter, $[m]$.
L	Pipe length, $[m]$.
S	Wetted perimeter, $[m]$.
A	Cross-sectional area, $[m^2]$.
$\mathbf{Q}$	Numerical vector of variables.
$\mathbf{L}$	Numerical operator.
$\mathbf{s}$	State vector.
v	General parameter.
$\mathbf{w}$	Gaussian noise.
$\mathbf{W}$	Covariance matrix.
M	Ensemble number.
$\mathbf{T}$	Covariance factor.
$\mathbf{P}$	Approximated covariance matrix.
$\mathbf{z}$	Measurements vector.
$\mathbf{R}$	Measurements covariance matrix.
$\mathbf{H}$	Selector matrix.
$\mathbf{K}$	Kalman gain.

Sub/superscripts

k	General phase.
g	Gas phase.
l	Liquid phase.
i	Interface.
s	Superficial.
0	Reference or initial.

h Hyperbolic.
i Cells index i.
n Time index n.
j Ensemble index j.

INTRODUCTION

Multiphase flows have a relevant role in many engineering applications such as in oil and gas industries. The possibility to control and measure flow parameters in wellbore and pipelines can strongly reduce costs and make growing production rate. However, real-time measurements along a wellbore or a pipe are often expensive and complex to realize. Therefore, in the last years, substitute methods to optimize and manage wellbore mining or pipeline transport process have reached a great importance and development.
Among these replacement methods, multiphase soft-sensors allow to estimate flow rates and flow parameters from cheap probes easy to place along a pipe, such as pressure gauges, combined with dynamic mathematical and numerical model. A great variety of soft-sensing techniques is available (often called data assimilation methods), as briefly explained by (Gryzlov *et al.*, 2010). According to them, two approaches are possible to soft-sensing: variational data assimilation methods, that use a minimization of a cost function, and sequential methods which, by a filtering technique, update the state of a system every time measurements are available. A widely used filtering technique is Kalman filtering, see (Kalman, 1960), initially developed for linear models and then derived into some extensions, such as the extended Kalman filter and the ensemble Kalman filter, suitable also for more complex and non-linear problems.
In the last decade, although soft-sensing techniques have not been widely employed in multiphase flow applications in pipes, some few important works have been presented on this topic. (Lorentzen *et al.*, 2003) applied the ensemble Kalman filter to the estimation of flow and closure parameters by a drift-flux model in a two-phase flow; then, the possibility to estimate both flow rate and parameters through the extended Kalman filter, applied to a drift-flux model, was discussed in (Leskens *et al.*, 2008). (Gryzlov *et al.*, 2010) presented an application of the ensemble Kalman filter, in combination, once again, with a drift-flux model, to estimate inflow along an horizontal wellbore under stratified conditions by measuring only pressure along the pipe and the other characteristics at the outlet section. Recently, a further application of the extended Kalman filter has been presented in (Gryzlov *et al.*, 2013), this time combined to the simplified no-pressure wave model, in order to estimate inflow along a horizontal pipe.
In this work, we try to extend the soft-sensing scheme presented by (Gryzlov *et al.*, 2010) to a more complex two-fluid model. (Ferrari *et al.*, 2017) developed a numerical scheme for a five equation, one-dimensional, hyperbolic two-fluid model able to capture transitions from stratified to slug flow. Here, this scheme is adopted in combination with an ensemble Kalman filter in order to create a soft-sensor model for flow estimations in horizontal pipe. First of all, the final objective is the estimation of inlet flow rates, knowing only pressure measurements along the pipe and outlet quantities. Then, the same technique is applied to a first attempt of estimation of a variable pipe diameter along the pipe, which can represents obstructions or constrictions in the pipe due, for example, to wax deposition. This phenomenon, in actual pipelines, can create issues and reduce the efficiency of hydrocarbon transportation and it is often difficult to predict, except through invasive and expensive inspections. So, the possibility to estimate this type of phenomenon using real-time dynamical numerical model, through only few easy and cheap measurements, can achieve a relevant importance in the optimization of multiphase flow industrial process.
For the applications presented here, the same five equation model by (Ferrari *et al.*, 2017) is kept also as reference system for actual values to be estimated and from which take pressure and outlet measurements.
The paper is organized as follows: first, the five equation model and its numerical solution are briefly recalled; then, the ensemble Kalman filter adopted is presented. Finally, before conclusion, results are shown, both for the inlet flow rate and for the diameter estimation.

MODEL AND NUMERICAL SCHEME

Model

In this paper, to describe a two-phase flow, we adopt the five equation, hyperbolic, one-dimensional, two-fluid model widely investigated by (Ferrari *et al.*, 2017). The flow is assumed to be isothermal; hence, the energy equations are not accounted for. The model consists in five time-dependent partial differential equations, four obtained from the conservation of mass and momentum for each phase. A fifth equation is added to the system: it expresses the evolution of the gas volume fraction. The system reads

$$\frac{\partial \alpha_g}{\partial t} + u_i \frac{\partial \alpha_g}{\partial x} = r_p(p_{ig} - p_{il}) \tag{1}$$

$$\frac{\partial (\alpha_g \rho_g)}{\partial t} + \frac{\partial (\alpha_g \rho_g u_g)}{\partial x} = 0 \tag{2}$$

$$\frac{\partial (\alpha_l \rho_l)}{\partial t} + \frac{\partial (\alpha_l \rho_l u_l)}{\partial x} = 0 \tag{3}$$

$$\frac{\partial (\alpha_g \rho_g u_g)}{\partial t} + \frac{\partial (\alpha_g \rho_g u_g^2)}{\partial x} + \alpha_g \frac{\partial p_{ig}}{\partial x} + \rho_g \alpha_g g \frac{\partial h}{\partial x} \cos(\theta) = - \rho_g \alpha_g g \sin(\theta) - F_{gw} - F_i \tag{4}$$

$$\frac{\partial (\alpha_l \rho_l u_l)}{\partial t} + \frac{\partial (\alpha_l \rho_l u_l^2)}{\partial x} + \alpha_l \frac{\partial p_{il}}{\partial x} + \rho_l \alpha_l g \frac{\partial h}{\partial x} \cos(\theta) = - \rho_l \alpha_l g \sin(\theta) - F_{lw} + F_i. \tag{5}$$

where the subscripts l and g stand for liquid and gas phase, respectively, interfacial variables have the subscript i and the subscript w indicates the wall. α is the volume fraction, ρ is density, u stands for phase velocity and p for pressure; p_{ig} and p_{il} indicate gas and liquid interfacial pressures; θ is the inclination angle, see Fig. 1, and g is the gravity acceleration. The F terms are the frictional forces per unit volume: they need closure relations, which are introduced at the end of this Section. Finally, h is the height of the liquid surface, as shown in Fig. 1. Pressure formulation derives from the average pressure value at each phase in stratified conditions, as shown by (Brauner and Maron, 1992). Finally, the equations are complemented by $\alpha_g + \alpha_l = 1$.
Thanks to the addition of the further Eq. (1), the five equation system becomes hyperbolic. Eq. (1) needs a closure relation for the interfacial velocity: (Saurel and Abgrall, 1999) proposed to estimate it as the velocity of the centre of mass

$$u_i = \frac{\sum \alpha_k \rho_k u_k}{\sum \alpha_k \rho_k}. \tag{6}$$

The right-hand side of Eq. (1), in which the pressure relaxation parameter r_p appears, takes into account the instantaneous pressure relaxation process. More details about instantaneous pressure relaxation process are discussed in (Ferrari

et al., 2017), (Saurel and Abgrall, 1999), and (Munkejord and Gran, 2009).
The five-equation system (1) - (5), with instantaneous pressure relaxation, provides a strictly hyperbolic alternative to the traditional four-equation two-fluid model and it is suitable for slug capturing, as shown and discussed in (Ferrari *et al.*, 2017).

Equations of State (EOS)

In the model adopted here, liquid and gas phases are both assumed to be compressible, hence the balance Eqs. (1) - (5) must be complemented with the equation of state (EOS) of each phase

$$p_{ik} = c_k^2(\rho_k - \rho_{k,0}) - p_0, \tag{7}$$

which relates pressures to densities; c_k is the speed of sound in phase k, $\rho_{k,0}$ is the reference density and p_0 is the reference pressure.

Closure models

The closure relations for the liquid-wall F_{lw}, gas-wall F_{gw} and interfacial F_i shear forces are defined as

$$F_{lw} = \frac{\tau_{lw} S_l}{A}, \qquad F_{gw} = \frac{\tau_{gw} S_g}{A}, \qquad F_i = \frac{\tau_i S_i}{A}, \tag{8}$$

where, see Fig. 1, A is the cross-section area, S_l, S_g stand for the perimeters wetted by the liquid and gas phases, respectively, and S_i is the cross section of the interfacial surface between the two phases.
Shear stresses τ are expressed as

$$\tau_{lw} = \frac{1}{2} f_{lw} \rho_l |u_l| u_l, \qquad \tau_{gw} = \frac{1}{2} f_{gw} \rho_g |u_g| u_g, \qquad \tau_i = \frac{1}{2} f_i \rho_g |u_g - u_l| (u_g - u_l). \tag{9}$$

In this work, we adopt the same friction factors formulation adopted by (Issa and Kempf, 2003) and (Ferrari *et al.*, 2017). For the gas-wall friction factors and for interfacial friction factors the correlations used for turbulent flow are

$$f_g = \begin{cases} \dfrac{16}{Re_g} & \text{if } Re_g < 2100, \quad (10a) \\ 0.046(Re_g)^{-0.2} & \text{if } Re_g \geq 2100; \quad (10b) \end{cases}$$

$$f_i = \begin{cases} \dfrac{16}{Re_i} & \text{if } Re_i < 2100, \quad (11a) \\ 0.046(Re_i)^{-0.2} & \text{if } Re_i \geq 2100. \quad (11b) \end{cases}$$

For liquid wall friction force we use

$$f_l = \begin{cases} \dfrac{24}{Re_l} & \text{if } Re_l < 2100, \ (12a) \\ 0.0262(\alpha_l Re_{sl})^{-0.139} & \text{if } Re_l \geq 2100. \ (12b) \end{cases}$$

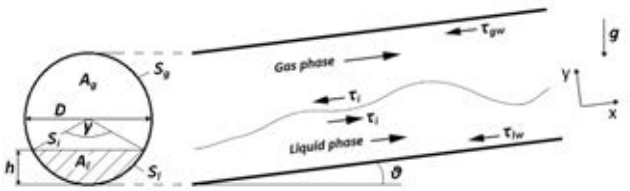

Figure 1: Geometry.

The Reynolds numbers are defined as

$$Re_g = \frac{4 A_g u_g \rho_g}{(S_g + S_i)\mu_g}, \qquad Re_i = \frac{4 A_g |u_g - u_l| \rho_g}{(S_g + S_i)\mu_g}, \qquad Re_l = \frac{4 A_l u_l \rho_l}{S_l \mu_l}, \qquad Re_{sl} = \frac{D u_{sl} \rho_l}{\mu_l}, \tag{13}$$

where, as indicated in Fig. 1, D is the pipe diameter, A_g and A_l are the pipe cross section occupied by the gas and liquid phase, respectively; μ is the dynamic viscosity and u_{sl} stands for the superficial liquid velocity.

Numerical method

Following previous works by (Ferrari *et al.*, 2017) and (Munkejord and Gran, 2009), Eqs. (1) - (5) are discretised on a uniform one-dimensional grid, by a finite volume method and a first order explicit time discretisation. The numerical solution is obtained through a succession of operators in a fractional-step process

$$\mathbf{Q}_i^{n+1} = \mathbf{L}_s^{\Delta t} \mathbf{L}_h^{\Delta t} \mathbf{Q}_i^n \tag{14}$$

where $\mathbf{Q}_i^n$ stands for the numerical approximation of the vector of variables in the cell i at time n and $\mathbf{Q}_i^{n+1}$ is the same vector at time $n+1$. Therefore, the solution is updated, at each numerical iteration, in two sequential sub-steps.
In the first sub-step, the hyperbolic operator $\mathbf{L}_h^{\Delta t}$ is applied, in each control volume i, to solve the hyperbolic system containing non-conservative terms

$$\frac{\partial \mathbf{q}}{\partial t} + \mathbf{A}(\mathbf{q}) \frac{\partial \mathbf{q}}{\partial x} = 0. \tag{15}$$

This requires the solution of the linear Riemann problem at interface of each cell, by a Roe method, and leads to an upwind resolution of the wave phenomena appearing in the problem. The solution of the Riemann problem is obtained basing on the high-resolution *Roe5* solver by (Munkejord and Gran, 2009). To solve the hyperbolic system (15), at each iteration, the value of the unknown vector $\mathbf{Q}_i^{h,n+1}$ is computed using a high resolution extension of Godunov's method. The use of a high resolution correction guarantees a second order accuracy in space.
In (Ferrari *et al.*, 2017) the *Roe5* scheme is modified to take into account the pressure terms for stratified flow, shear forces, and transition from two (i.e. stratified flow) to one phase (i.e. slug flow).
Finally, in a second sub-step, the operator $\mathbf{L}_s^{\Delta t}$ is applied to add source terms, appearing in momentum Eqs. (4) - (5), and to take into account the pressure relaxation process.
As pointed out by (Munkejord and Gran, 2009) and (Ferrari *et al.*, 2017), the five equation system with instantaneous pressure relaxation can be adopted as an alternative numerical method to solve the four-equation two-fluid model, gaining the hyperbolicity.
Since in a slug capturing process, during the slug onset process, the transition from two-phase flow to single phase flow occurs, the liquid volume fraction grows and tends to unity; conversely, gas volume fraction tends to zero and this generates numerical problems as discussed by (Munkejord and Gran, 2009). Ferrari et al. (Ferrari *et al.*, 2017) introduce a slug criterion to handle these numerical issues.
This numerical method is implemented in a code called ***5ES-CARGOTS***. Details are discussed in (Ferrari *et al.*, 2017).

ENSEMBLE KALMAN FILTER

To solve the inverse problem, since the system of Eqs. (1) - (5) adopted in this work is non-linear, we need to use the *ensemble Kalman filter* (EnKF), an extension of the Kalman filter. This filter has been used by (Gryzlov *et al.*, 2010) and (Lorentzen *et al.*, 2003) in their works.
The main difference between EnKF and traditional Kalman filter is how the error covariance matrix is calculated. The ensemble Kalman filter calculates the approximation of the covariance matrix using an ensemble of model forecasts. The members of the ensemble can be generated randomly from a Gaussian distribution, as done in (Gryzlov *et al.*, 2010).
First, a state vector is introduced

$$\mathbf{s} = [\alpha_{l,i}\ u_{g,i}\ u_{l,i}\ p_i\ v_i]^T \tag{16}$$

where the primitive variable α_l, u_g, u_l and p are extrapolated, each time the filter is used, from the numerical solution of the five equation system (1) - (5), in which the values of the two densities are rounded up in the common value of pressure p. The subscript i is the cell index of the numerical discretization. If the final purpose is also the estimate of model parameters, these are accounted for in the generic variable v.
In order to initialize the filter, the initial ensemble of the state vector is generated (for semplicity, the cell index i is omitted)

$$\mathbf{s}_{0,j} = \bar{\mathbf{s}}_0 + \boldsymbol{w}_{0,j} \tag{17}$$

where j indicates the j'th member of the ensemble, $\bar{\mathbf{s}}_0$ is the initial mean state vector and $\boldsymbol{w}_{0,j}$ is a Gaussian noise with zero mean.
So, the state vector is estimated through a recursive scheme, composed by the following two steps:

1. **forecast step** - the direct model is run one time step forward for each member of the ensemble obtaining the updated forecast state vector

$$\mathbf{s}^-_{n,j} = \chi(\bar{\mathbf{s}}_{n-1,j}) + \boldsymbol{w}_{n,j} \tag{18}$$

where $\boldsymbol{w}_{n,j}$ corresponds to the model error covariance matrix $\mathbf{W}_n$, n denotes the time step and χ is the model's numerical solution function.
The model error is usually added only to the components of the state vector $\mathbf{s}$ that have more uncertainty on their values, as in the case of parameters or input quantities.
Then, through the mean value of the state vector

$$\bar{\mathbf{s}}^-_n = \frac{1}{M}\sum_{j=1}^{M} \mathbf{s}^-_{n,j} \tag{19}$$

and the factor

$$\mathbf{T}^-_n = \frac{1}{\sqrt{M-1}}[(\mathbf{s}^-_{n,1} - \bar{\mathbf{s}}^-_n), (\mathbf{s}^-_{n,2} - \bar{\mathbf{s}}^-_n), \ldots, (\mathbf{s}^-_{n,M} - \bar{\mathbf{s}}^-_n)] \tag{20}$$

we obtain the error covariance matrix

$$\mathbf{P}^-_n = \mathbf{T}^-_n (\mathbf{T}^-_n)^T \tag{21}$$

where M is the number of the members of the ensemble;

2. **analysis step** - measurements $\mathbf{z}_{n,j}$, distributed with known variances, are take into account. As pointed out by (Gryzlov *et al.*, 2010), assuming that measurement errors are statistically independent, the measurements covariance matrix $\mathbf{R}$ is diagonal and constant. The matrix $\mathbf{H}$ is used to select data or physical characteristics from the actual system to obtain the measurements that will be compared to the corresponding values of the forecast state vector, as follows

$$\mathbf{z}_n = \mathbf{H}_n \mathbf{s}_n + \boldsymbol{\upsilon}_n \tag{22}$$

where $\boldsymbol{\upsilon}_n$ is the measurement Gaussian error identified by the covariance matrix $\mathbf{R}$.
Therefore the Kalman gain is calculated as follows

$$\mathbf{K}_n = \mathbf{P}^-_n \mathbf{H}^T (\mathbf{H}\mathbf{P}^-_n \mathbf{H}^T + \mathbf{R})^{-1} \tag{23}$$

and the analyzed state for each member of the ensemble is given by

$$\mathbf{s}_{n,j} = \mathbf{s}^-_{n,j} + \mathbf{K}_n(\mathbf{z}_{n,j} - \mathbf{H}\mathbf{s}^-_{n,j}). \tag{24}$$

Finally, the mean value of the analyzed ensemble is

$$\bar{\mathbf{s}}_n = \frac{1}{M}\sum_{j=1}^{M} \mathbf{s}_{n,j}. \tag{25}$$

and it represents the best estimate of the actual system.

Now, the cycle can restart from the step 1.
To avoid poor quality performances of the filter due to truncation errors, since variables involves in the Kalman filtering process can have different orders of magnitude, the variables in the state vector $\mathbf{s}$ have to be adimensionalized on some reference values $\mathbf{s}_{ref}$, as suggested by (Gryzlov *et al.*, 2010)

$$\mathbf{s}_{ad} = \mathbf{s}/\mathbf{s}_{ref}, \tag{26}$$

obtaining the adimensionalized state vector $\mathbf{s}_{ad}$ in which quantities have the same order of magnitude. In this work, the reference values are ones assumed by the variables of the problem in the last cell of the discretized geometries, corresponding to the outlet section. Therefore

$$\mathbf{s}_{ref} = [\alpha_{l,o}\ u_{g,o}\ u_{l,o}\ p_o\ v_o]^T, \tag{27}$$

where the subscript o stands for outlet. The same procedure is applied to the measurement vector $\mathbf{z}$.

RESULTS

Flow rate estimate

In a first test case we try to estimate inlet flow rates in slug flow conditions. First, using the 5ESCARGOTS code by (Ferrari *et al.*, 2017), we simulate an air/water two-phase flow reference problem in a horizontal pipe to keep as actual system to be estimated. The pipe is 36 m long with a diameter equal to 0.078 m. The simulation starts with stratified conditions; inlet superficial velocities are chosen to guarantee that slug flow conditions will develop during the simulation. Therefore, gas and liquid superficial velocities are fixed to 2.0 m/s and 1.5 m/s, respectively. Cells number is set to 900, corresponding to a CFL condition of 0.25. Outlet is open to ambient pressure. The liquid phase is water ($\mu_l = 1.14 \cdot 10^{-3}\ Pa \cdot s$, $\rho_{0,l} = 1000.0\ kg/m^3$) and the gas phase is air ($\mu_g = 1.79 \cdot 10^{-5}\ Pa \cdot s$, $\rho_{0,g} = 1.0\ kg/m^3$). In Fig. 2 the liquid volume fraction profile along the pipe after 8 s of simulation is reported: it is clearly visible a slug in the second half of the pipe.
Then, by the combination of the same 5ESCARGOTS code

with an ensemble Kalman filter, a soft-sensing scheme is implemented in order to estimate actual inlet flow rate (i.e. inlet superficial velocities of the first simulation) starting from a initial guess, for example 1.0 m/s for both gas and liquid superficial velocities. The state vector, in this case, is defined as

$$\mathbf{s} = [\alpha_{l,i}\ u_{g,i}\ u_{l,i}\ p_i]^T \tag{28}$$

where inlet superficial velocities are extrapolated directly from the left boundary condition. The ensemble Kalman filter is inizialized by gaussian errors based on standard deviations about 1% of the value of the characteristics of the state vector **s**.

In a first test, we run a soft-sensor with the so-called twin simulation, see (Gryzlov *et al.*, 2010), i.e. a simulation with the same conditions of the actual one, except for inlet superficial velocities. Inlet conditions are estimated through measurements of pressure in each cell along the pipe and by the measure of the other characteristics at the outlet section every 0.25 s.

Figure 3 shows the estimated inlet superficial velocities compared to the actual values of the first simulation: the soft-sensor, with the ensemble number set to 100, estimates very well actual values for both phases, also when slug flow arises and develops, i.e. after about 5 seconds of simulation. On the other hand, the great number of pressure measurements used in this case is unrealistic for an application.

If we try to reduce the number of numerical pressure gauges along the pipe, the soft-sensor system becomes quickly unstable, due probably to the great number of unknown that characterized the five equation model adopted, if compared to the number of measurements chosen to use here.

Therefore, in a second test case, we decide to run the soft-sensor reducing the number of cell to 36, measuring pressure from the actual simulation only in the 36 positions along the pipe, corresponding to the centre of each of the 36 cells used in the soft-sensor. If that, on one hand, leads to a more poor physical description of the slug phenomenon, it allows, on the other hand, to reduce computational costs and the number of pressure measurements along the pipe, making the soft-sensor more suitable for real application.

Figure 4 shows results in the case of 36 pressure measurements. It is clearly visible that the estimate is very good only for the first five seconds of simulation, i.e. when the flow is stratified. Then, when slug conditions arise (after about 5 seconds of simulation, as indicated in Fig. 4), estimates leave the actual values and the estimate error becomes a little higher, in the order of 5-10%. This fact is due to the inadequate description of the slug flow since the number of cells is insufficient. Therefore, in future applications, a better compromised between the accuracy in the simulation of the physical phenomena and the efficiency of the soft-sensing technique would be investigated.

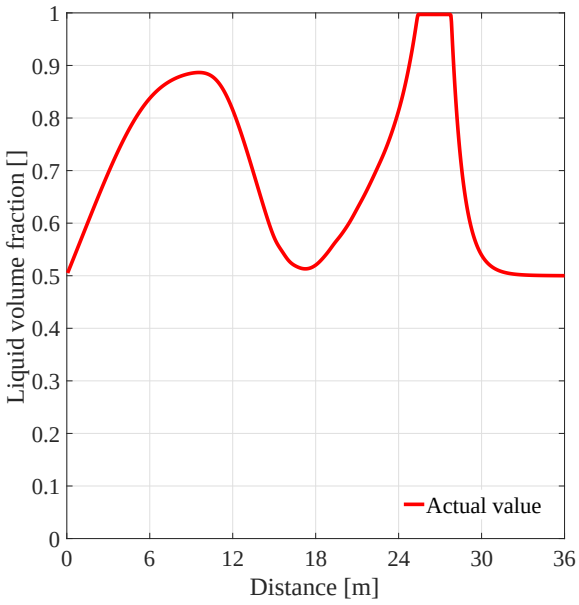

Figure 2: Slug flow after 8 s of simulation. Liquid volume fraction profile.

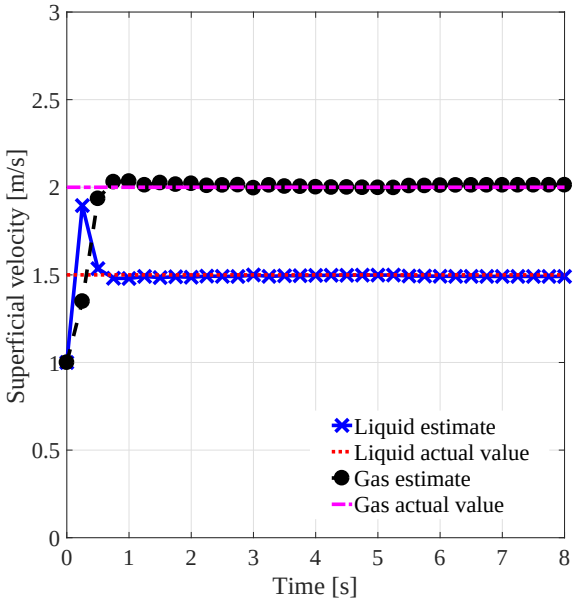

Figure 3: Inlet flow rate estimation by pressure measurements in every cell along the pipe.

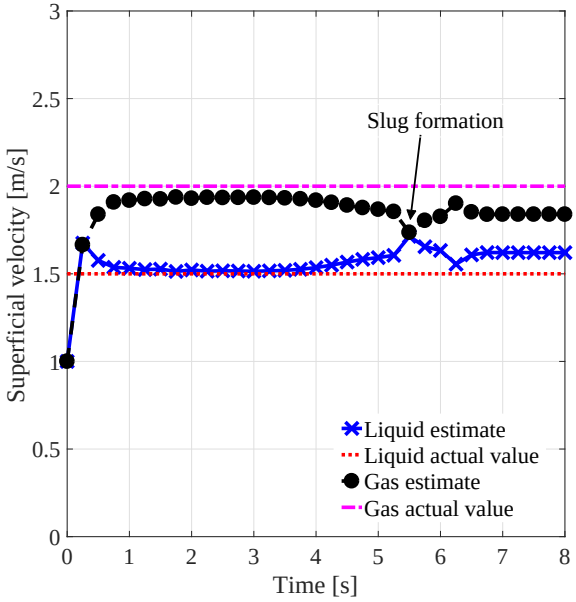

Figure 4: Inlet flow rate estimation by 36 pressure measurements along the pipe.

Diameter estimate

In actual pipelines, wax deposition can create obstructions or constrictions reducing the efficiency of hydrocarbon transportation. This phenomenon is often difficult to predict, except through invasive and expensive inspections. Therefore, the possibility to estimate the entity and the position of a potential obstructions along a pipe, using real-time dynamical numerical model, through only few easy and cheap measurements, can be very important in the optimization of multiphase flow industrial process.
This can be obtained, through a soft-sensing technique, considering the diameter not as a constant parameter but as a variable, that can assume, at the same instant, N possible different values, where N is the number of cells, taking into account the presence of potential reduction of the local cross-section.
Therefore, the same technique presented in the previous Section is here applied to a first attempt of estimate of a variable pipe diameter along the pipe. Geometrical and flow conditions are the same of the previous test case, but now the unknowns to be estimated are not inlet flow conditions but the values of a variable diameter along the pipe. So the state vector, in this case, becomes

$$\mathbf{s} = [\alpha_{l,i}\ u_{g,i}\ u_{l,i}\ p_i\ d_i]^T, \tag{29}$$

where d_i are the different diameters in the cells.
First of all, a simulation with a constant diameter, set to the value of 0.078 m, is run and it is kept as actual reference for the following estimate process. Then, by the use of an ensemble Kalman filter, a soft-sensor simulates the same test case but with a diameter value expressed for each cell. As initial guess, the soft-sensor starts with a distributed diameter with same value in each cells, fixed to 0.13 m, to which is added a Gaussian noise.
Preliminary tests have showed that the estimate of non constant diameter makes the soft-sensor unstable and not efficient. In fact, as pointed out by (Gryzlov *et al.*, 2010), the attempt to estimate parameters, in particular if their number is large, as in this case, increases the size of the state vector $\mathbf{s}$, in which the variable diameter must be included. This leads to a dramatical decreasing of the robustness of the method. Therefore, as first attempt, we decide to include among measurements to be used for the estimate process, beside pressure values, also liquid volume fraction values along the pipe, in order to decrease the great disparity between the size of the state vector and the number of the available measurements. Obviously, this compromise is quite unrealistic for actual applications, but it allows us to obtain and discuss some first results. As for the inlet flow rate estimate, soft-sensor is set to a cell number equal to 36.
Figure 5 shows the estimated diameter along the pipe at different times in comparison with the actual diameter value. The estimate quickly reaches the actual value along all the pipe in the first seconds of simulation, i.e. when the flow is stratified; then, after the development of the first slug, the estimate becomes less accurate, with significant oscillations.

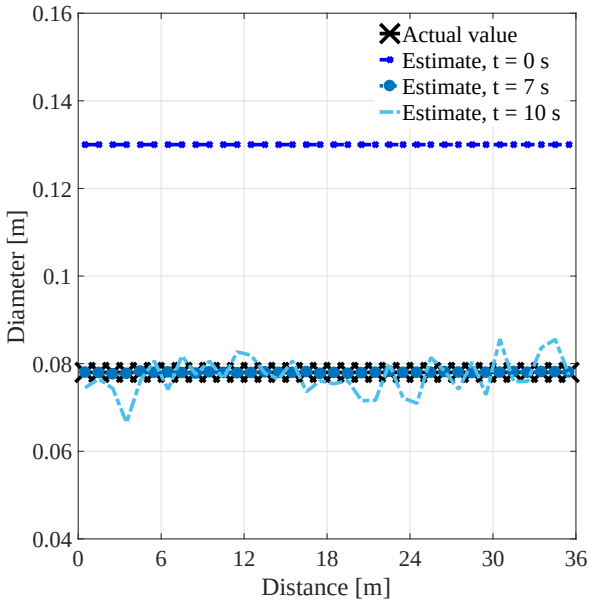

Figure 5: Diameter estimate along the pipe at three different time instants.

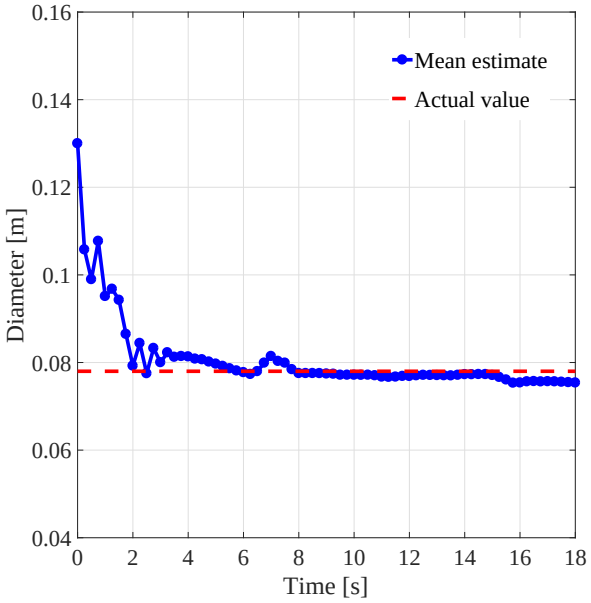

Figure 6: Mean diameter estimate during simulation.

In Fig. 6 the profile of the estimate of the mean diameter during the simulation, calculated along cells, is compared to the actual value. In this last case, the less accuracy of the soft-sensor when the flow is under slug regime is less visible. This results lead to the conclusion that the estimate of a variable diameter along the pipe is feasible also under slug flow conditions; however, the five equation model adopted here seems to be too complex for a soft-sensing application, since the great size of the state vector badly affects the filter accuracy.

CONCLUSION

In this paper, a soft-sensing technique, composed by a five equation two-fluid model and an ensemble Kalman filter, is presented. The 5ESCARGOTS code, numerically developed for slug capturing purposes by (Ferrari *et al.*, 2017), guarantees to capture the transition from stratified to slug flow; here it is combined with an ensemble Kalman filter, in order to estimate real-time inlet flow rate and variable diameter along the pipe, using the less possible number of measurements from the actual system.
Results shows estimate in quite good agreement with actual

values, but they demonstrate also some limits of the soft-sensor presented in this paper. In fact, this work leads to the conclusion that the estimate of inlet flow rate and variable diameters along the pipe seems to be feasible also under slug flow conditions; however, in some cases, the five equation model appears too complex for a soft-sensing application since the great size of the state vector badly affects the filter accuracy. In future applications, a better compromised between the accuracy of the slug phenomenon simulation and the efficiency of the soft-sensing technique would be investigated.

REFERENCES

BRAUNER, N. and MARON, D.M. (1992). "Stability analysis of stratified liquid-liquid flow". *Int. J. Multiph. Flow*, **18**, 103–121.

FERRARI, M., BONZANINI, A. and POESIO, P. (2017). "A five-equation, transient, hyperbolic, one-dimensional model for slug capturing in pipes". Accepted for publication in *Int. J. Numer. Meth. Fluids*.

GRYZLOV, A., SCHIFERLI, W. and MUDDE, R.F. (2010). "Estimation of multiphase flow rates in a horizontal wellbore using an ensemble kalman filter". *Proc. 7th Int. Conf. on Multiph. Fl.* ICMF2010, Tampa, FL USA.

GRYZLOV, A., SCHIFERLI, W. and MUDDE, R.F. (2013). "Soft-sensors: model-based estimation of inflow in horizontal wells using the extended kalman filter". *Flow Meas. Instrum.*, **34**, 91–104.

ISSA, R.I. and KEMPF, M.H.W. (2003). "Simulation of slug flow in horizontal and nearly horizontal pipes with the two-fluid model". *Int. J. Multiph. Flow*, **29**, 69–95.

KALMAN, R.E. (1960). "A new approach to linear filtering and prediction problems". *J. Basic Eng.*, **82**, 35–45.

LESKENS, M., DE KRUIF, B., BELFROID, S., SMEULERS, J. and GRYZLOV, A. (2008). "Downhole multiphase metering in wells by means of soft-sensing". *Proc. SPE Intel. Energy Conf. and Exhib.* Amsterdam, The Netherlands.

LORENTZEN, R.J., NAEVDAL, G. and LAGE, A.C.V.M. (2003). "Tuning of parameters in a two-phase flow model using an ensemble kalman filter". *Int. J. Multiph. Flow*, **29**, 1283–1309.

MUNKEJORD, S.T. and GRAN, I.R. (2009). *Modelling and numerical methods for two-phase flow*, vol. Phd Thesis 2005, NTNU, Trondheim, Norway. VDM Verlag Dr. Müller Aktiengesell & Co. KG, Saarbrücken, Germany.

SAUREL, R. and ABGRALL, R. (1999). "A multiphase godunov method for compressible multifluid and multiphase flow". *J. Comput. Phys.*, **150**, 425–467.